

We are IntechOpen, the world's leading publisher of Open Access books Built by scientists, for scientists

6,900

Open access books available

185,000

International authors and editors

200M

Downloads

Our authors are among the

154

Countries delivered to

TOP 1%

most cited scientists

12.2%

Contributors from top 500 universities



WEB OF SCIENCE™

Selection of our books indexed in the Book Citation Index
in Web of Science™ Core Collection (BKCI)

Interested in publishing with us?
Contact book.department@intechopen.com

Numbers displayed above are based on latest data collected.
For more information visit www.intechopen.com



New Generation of High Efficient OLED Using Thermally Activated Delayed Fluorescent Materials

Manish Kumar, Miguel Ribeiro and Luiz Pereira

Additional information is available at the end of the chapter

<http://dx.doi.org/10.5772/intechopen.76048>

Abstract

The search for efficient materials for organic light emitting diodes is one of the most imperative research area. The focus is to obtain a bright large area emitter, limited by the low internal quantum efficiency of conventional organic emitters. Recently, a new generation of the organic materials (TADF) with a theoretical internal quantum efficiency up to 100%, opened new frameworks. However, significant challenges persist to achieve full understanding of the TADF mechanism and to improve the OLEDs stability. Starting from the photo-physical analysis, we show the relationship with the molecular electrical carrier dynamics and internal quantum efficiencies. The OLED structure, fabrication, and characterization are also discussed. Several examples for the full color emitters are given. Special emphasis on experimental results is made, showing the major milestones already achieved in this field.

Keywords: organic light emitting diodes, thermally activated delayed fluorescence, photoluminescence, electroluminescence, triplet harvesting

1. Introduction

Since the first invention of the organic light emitting diodes (LEDs) in 1987 by Tang and Van Slyke [1] that represented an advancement in display and lightening technologies, Organic light-emitting diodes (OLEDs) have emerged as an extensive active field in the both scientific as well technological aspects. Organic light-emitting diodes (OLEDs) are cheap, flexible, and cheap like a movie projector screen. They have attracted considerable attention due to their promising applications in cheap, energy-saving, eco-friendly and solid-state lighting [2–4].

The current research in OLEDs is emerging technology which is also a growing market and expected to cross 20 billion by 2030 [5]. OLEDs are used in several flat and roll displays, also in white LEDs for the lighting. OLEDs give freedom of taking advantage of emission in different colors, color modulation (color coordinates, temperature and color rendering—white lighting), diffused light—(light from flat panels (large area) and high viewing angle), Freedom design (thin, lightweight, flexible transparent—easy incorporation into 3D surfaces), etc. Along with these characteristics, there is some difficulty in getting a large homogeneous emitter area, where the organic materials rapidly degrade in the presence of oxygen and/or humidity. Although solved with rigid OLEDs, flexible ones have low lifetime (no efficient encapsulation system has been developed). The main principle behind OLED technology is electroluminescence and such devices offer brighter, thinner, high contrast, and flexibility.

In the conventional OLEDs, the materials used are π -electron-rich molecules, which helps in the fast charge transfer at the interface. But in these OLEDs, the internal quantum efficiency (IQE) is lower which results to the lower external quantum efficiency (EQE) of 5% and limits the OLEDs development because of the nonradiative triplet exciton non-harnessing. Usually, materials used for OLEDs are phosphorescent emitters such as iridium [6–8] or platinum complexes [9, 10] that are used to achieve the electroluminescence efficiency. In such systems, both 25% singlet excitons and 75% triplet excitons can be used for harnessing the electroluminescence. In phosphorescent OLEDs, the internal quantum efficiency was reported close to 100% [11–16], but the disadvantage in such phosphorescent material is their high cost and poor stability. Along with phosphorescent material harnessing phosphorescence [7, 17], triplet-triplet annihilation [18] were also used. Therefore, to achieve 100% low-cost IQE, the development of an alternative to harvest the 75% triplet exciton is important for the future of OLEDs. In this context, response to this need, the development of the thermally activated delayed fluorescence (TADF) materials with the most promising exciton harvesting mechanism used in OLED devices, which was firstly reported by Adachi et al. in [19] received tremendous attention, and in recent years, considerable efforts have been devoted towards the fabrication of OLEDs based on TADF materials where the IQE can be easily achieved up to 100% [20, 21].

In this chapter, we summarize the fundamentals of thermally activated delayed fluorescence process, their optoelectronic behavior linking with the device performance and recent experimental studies of the introduction of TADF emitters used as the doping/guest material for OLED fabrication. Along with, a summary of the best TADF emitters used for fabrication of orange-red, blue and green-yellow OLEDs is provided. In addition, a correlation is provided between the structure and doping percentage of TADF emitters and their optoelectronic properties.

2. Theory and concepts of thermally activated delayed fluorescence

The starting point to understand the TADF principle in organic luminescent materials is to consider the fundamental *sp* orbitals hybridization. The carbon–carbon (C–C) conjugation, employing two 2 *s*-orbital electrons and two 2*p*-orbitals electrons, leads to the *s* and *p* orbitals mix, giving place to three *sp* orbitals and one non-hybridized *p* orbital. The C–C

covalent bond is made using two *sp*. orbitals, from each carbon atom, giving rise to a usually called π bond; the third makes a covalent bond around the inter-nuclear axis and is usually called as σ bond. This simplified framework can explain the major electro-optical behavior of organic compounds. Effectively, whereas the π bonds located above and below (respectively, π^* - anti-bonding and π bond), originating an overlapping of the *sp*. orbitals in each side, the σ bond is a pure bond between two adjacent atoms. Besides the orbitals geometry, the electrical carriers are allowed to hopping among the $\pi\pi^*$ cloud, in contrary to σ carriers that are confined. The $\pi\pi^*$ cloud is the basic formation of the occupied and unoccupied energy levels and the further definition of HOMO (highest occupied molecular orbital) and LUMO (lowest unoccupied molecular orbital) levels. The σ energy region is typically a forbidden gap. From this simple configuration, organic molecule energy levels are typically singlet (S) and triplet (T) with the ground state a singlet S_0 [22]. The excited levels comprise, therefore, several S_n and T_n energy states, although in a simple model we may consider the first S_1 and T_1 excited levels. Under excitation (electrical and/or optical), the electrons are promoted to these excited levels, one in S_1 and three in T_1 . This is the main drawback of pure organic compounds: the de-excitation towards the S_0 ground state can be evaluated by the transition probability that is given by $\langle \psi_1 | r | \psi_0 \rangle$ where ψ_1 , ψ_0 and r are the wave-functions of the excited level and of the fundamental one, and r the electrical dipole quantum operator. By spin multiplicity rules, the $T_1 \rightarrow S_0$ transition is strictly forbidden and 75% of excited electrons can only relax by the nonradiative process, remaining only 25% of excited carriers available for the radiative (luminescent) transition $S_1 \rightarrow S_0$ (spin allowed). This means that the maximum internal efficiency of a pure organic luminescent material is only 25%. Overcoming this constraint is an absolute priority for achieving highly efficient organic electroluminescent devices. Besides the well-known transition metals organic-inorganic complexes [22] that promote a strong spin-orbit coupling (SOC) with further enhanced phosphorescence, several other paths have been considered. The most promising, and subject of this chapter, is the TADF materials.

The analysis of this process can be based on the exciton formation (electron-hole pair) in a conjugated organic material. An electronic charge can be transferred between both entities in a two molecules system (or also in different parts of the same molecule). This process is called of charge-transfer (donor-acceptor complex) leading origin to the CT energy levels. The primary effect of these levels is to provide an electrostatic attraction, stabilizing the molecule. But, interestingly, this CT state is spin selective and is supposed to be able to change the triplet / singlet balance, allowing a conversion of triplet excitons to singlet ones. Although being still an unclear mechanism, was the fundamental starting point to the TADF materials. The **Figure 1** shows, in a simple scheme, the fundamental process involved in the excitation / de-excitation of an organic molecule.

An efficient TADF emission needs to enhance the transition probability k_{rISC} ($T_1 \rightarrow S_1$) relatively to the K_{nrP} transition $T_1 \rightarrow S_0$. Moreover, the TADF efficiency is directly related with the $rISC$ transition probability, that, in turns, depends on the energy difference between the S_1 and T_1 states, ΔE_{ST} according to the following simple equation [23]:

$$k_{rISC} = A \exp\left(-\frac{\Delta E_{ST}}{k_B T}\right) \quad (1)$$

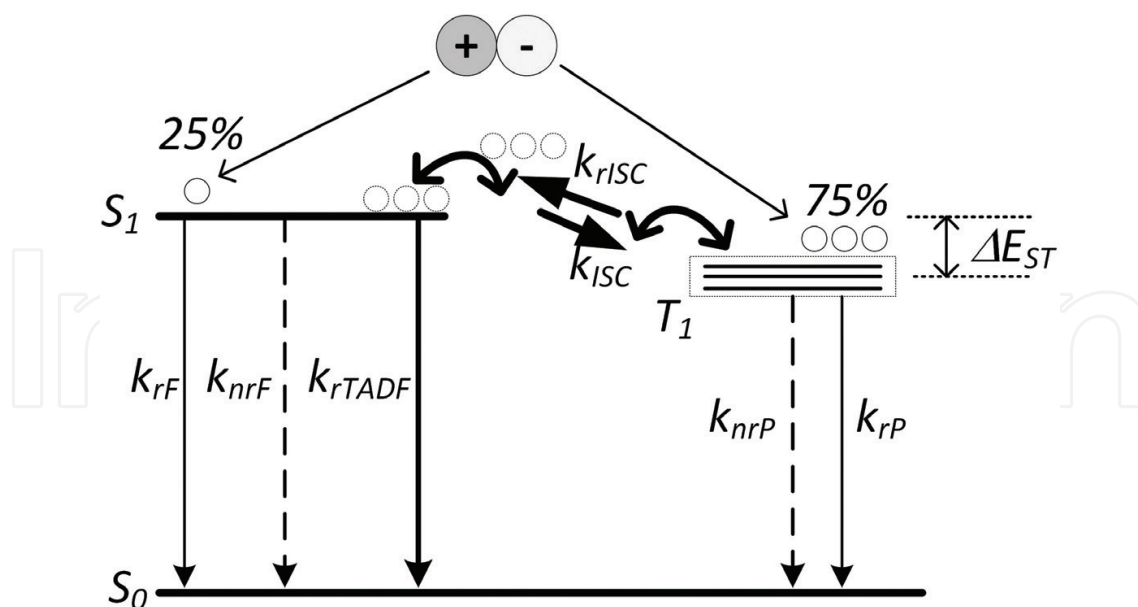


Figure 1. A simple scheme of the electroluminescence process involving an organic light emitter material. The transition probabilities (the inverse gives the transition lifetime) are k_{rF} , k_{rP} , k_{nrF} , k_{nrP} , k_{ISC} and k_{rISC} (radiative fluorescence, radiative phosphorescence, nonradiative, inter-system crossing and reverse inter-system crossing). TADF emission is related to k_{rTADF} and strictly depends on k_{rISC} .

where k_B is the Boltzmann constant, T the temperature and A the pre-exponential factor. The value of ΔE_{ST} naturally depends on the typical energy arising from the electrostatic interactions among the molecular orbitals. Particularly important, we need to consider the one-electron orbital energy in excited state (E) (supposing a fixed nuclear model), the typical electron repulsion energy (K) and the exchange energy (J) resulting from electron–electron repulsion based on the Pauli exclusion principle, affecting two excited unpaired electrons (one in LUMO and another one in HOMO levels) [24]. As the singlet and triplet excited states have a different spin ordering, the J value is usually higher in S_1 state and lower (in the same amount) in T_1 state [20]. With such consideration, the energy associated with the S_1 and T_1 states (respectively E_{S_1} and E_{T_1}) and therefore the ΔE_{ST} can be easily established, by the following relationships:

$$\begin{aligned} E_{S_1} &= E + K - J \\ E_{T_1} &= E + K - J \\ \Delta E_{ST} &= E_{S_1} - E_{T_1} \implies \Delta E_{ST} = 2J \end{aligned} \quad (2)$$

The immediate conclusion is that the minimization of ΔE_{ST} implies a lowest possible exchange energy. Remembering that the two unpaired electrons should be considered as distributed in the frontier orbitals of the LUMO and HOMO levels (T_1 or S_1 , excited states) resulting in pure LUMO-HOMO transitions, J can be given by [20]:

$$J = \iint \psi_L(r_1) \psi_H(r_2) \left(\frac{q^2}{r_1 - r_2} \right) \psi_L(r_2) \psi_H(r_1) dr_1 dr_2 \quad (3)$$

where ψ_H , ψ_L , r_1 , r_2 , and q are the HOMO and LUMO wave functions, the coordinate positions and electronic charge, respectively. From this equation, is very easy to verify that a minimization of J requires a negligible wave functions overlapping and therefore, a very low (or absence) of spatial overlapping between HOMO and LUMO levels (a spatial separation between HOMO and LUMO frontier orbitals). In a single molecule, this basic rule can be obtained if the molecule has independent structural moieties, one containing electron-donor (D) and another with electron-acceptor (A) which promotes the D-A charge transfer in the excited state. Therefore, the basic rule for an efficient *rISC* process in a single molecule is to guarantee if such molecule has at least, two unities (D and A, with non-overlapped orbitals) spatially separated. This can be achieved by increasing the spatial distance between such unities using a π -conjugated link or forcing a large dihedral angle between the planes of the donor and the acceptor, i.e. roughly speaking, forces a twist between D and A unities around the common axis [25]. In any case, we expect a strong CT character in the excited states.

The physical model to explain the *rISC* process is so far little understood. The first successful application [26] precisely focuses on the twisted D-A unities. In the first explanations, the CT states are used as a key to promoting the *rISC* process (singlet and triplet character, ^1CT and ^3CT). Following the known rules, the *ISC* (and therefore the *rISC*) process will be efficient under an occurrence of symmetry change of the excited states. This means in triplet/singlet systems, if a high value for k_{ISC} and k_{rISC} exist, T_1 and S_1 can be found in LE (local excited) and CT states respectively. However, we know that efficient TADF can occur even if such rule is not observed. Moreover, the excited states involved in TADF organic material, are typically a mixture of CT-LE states and not pure CT or LE states. Furthermore, extensive studies involving photoluminescence data reveal some discrepancies and new hypothesis involving also the LE states begin to be considered. In a general organic molecule (system), the excited states can be described in terms of their binding energy: the CT (low binding energies) and LE (strong binding energies). This LE has a very high radiative probability (with a strong emission) due to the high orbitals overlapping (the dipole electrical operator in the wave functions gives a high resulting probability). The *rISC* process model with only CT states starts to pose some problems with the discovery of SOC between such intramolecular states are zero [27]. Several hypotheses have been discussed and it was found that it is possible to tune independently two excited states involved in the *rISC* process [28] (for instance with different characters like ^1CT and ^3LE); or a more sophisticated model involving a mixture of ^3LE and ^3CT states [29] giving rise to an hypothesis where the *rISC* process depends on the SOC ($^3\text{LE} \rightarrow ^1\text{CT}$) and also on a hyperfine coupling induced *ISC* process ($^3\text{CT} \rightarrow ^1\text{CT}$). However, and in spite of an allowed SOC between these states, the calculations of the *rISC* probabilities (relatively low) cannot explain the experimental data that gives much higher values. Recently [30] a more complex model involving two steps was proposed. In such model, the first equilibrium between ^3LE and ^3CT states is promoted by vibronic coupling between them (also called as *rIC* – reserve intersystem crossing, helping the thermally assisted internal conversation); next, a coupling between the ^3CT and ^1CT states via ^3LE state (very efficient) promotes the *rISC* finalization process. In this model, both SOC and vibronic coupling are involved. All these models are, in general, well supported by several experimental data but at this moment, and depending on the specific organic emitter studied, different pathways need to be considered, leading to several open questions. In any case, this topic remains heavily investigated.

Besides the usual D-A molecule separated structure, some new molecules based on D-A-D (so-called “butterfly-shaped” structure) also exhibits TADF emission. Surprisingly, in several of such molecules, the energy gap between the lowest ^1CT state and the lowest ^3LE state (with $\pi \rightarrow \pi^*$ transition) are much higher than those found between ^1CT and ^3CT energy states in the conventional D-A molecules. The explanation was the two-step model above referred. This model appears to be the most interesting and well supported by experimental results.

Particularly important in this model, is the ability to modulate the energy of the excited ^1CT state via the environment polarity [31]. In solution, the photophysics analysis can help in revealing the main process involved, in turn, dependent on the solvent polarity. On film (solid state), this possibility opens a wide range of choice for the organic host material in order to significantly improve the efficiency of an OLED based on a TADF material. In a simple scheme, we can, therefore, represent the excited state of the TADF molecule as shown in **Figure 2**.

It must be noted that, according to this model, and following several experimental data (see [30] and references therein) the energy transfer SOC-ISC is more efficient in a D-A perpendicular geometry, in a transition $n\pi^*$ -like. This is a consequence of the maximum change in the orbital angular momentum as the SOC depends on the spin magnetic quantum number of the electrons and simultaneously on its spatial angular momentum quantum number (the SOC operator is proportional to $\hat{s} \cdot \hat{l}/\hbar^2$). Following this two steps model, the probabilities of k_{rIC} and k_{rISC} can be written in terms of both physical process involved [31]:

$$k_{rIC} = \frac{2\pi}{\hbar Z} \left| \langle \psi_{3CT} | \hat{H}_{SOC} | \psi_{3LE} \rangle \right|^2 \times \Delta(E_{3LE} - E_{3CT})$$

$$k_{rISC} = \frac{2\pi}{\hbar Z} \left| \frac{\langle \psi_{1CT} | \hat{H}_{SOC} | \psi_{3LE} \rangle \langle \psi_{3LE} | \hat{H}_{VIB} | \psi_{3CT} \rangle}{\Delta(E_{3LE} - E_{3CT})} \right|^2 \times \Delta(E_{3CT} - E_{1CT}) \quad (4)$$

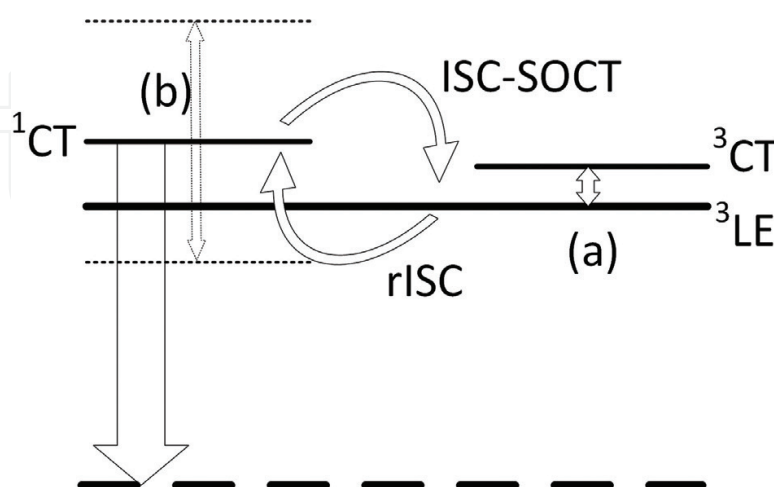


Figure 2. A simple representation of a TADF emitter in excited state, following the model proposed in [30]. In (a) the SOC-ISC transition is enhanced by vibronic coupling between the ^3CT and ^3LE states whereas in (b) the ^1CT state can be modulated by the environment polarity.

with Z being the canonical partition function for vibrational motion in the initial electronic state. These terms are therefore the starting point for a more detailed description of the TADF process. Knowing these probabilities, that we can estimate, several possibilities to further tuning the TADF process is possible. Despite several well-founded hypothesis, the fully understand of TADF process in organic emitters, still remains under major studies.

3. Fundamental photophysics of an organic TADF emitter

The starting point for developing an efficient OLED using TADF emitter is based on the luminescence properties of the emitter itself. As an earlier point, the physical process involved are not really straightforward, but leaving aside the pure photophysics process studies, the important figures of merit regarding efficiency can be easily obtained.

From **Figure 1**, we can formally consider two different kinds of radiative emissions arising in S_1 state: from its own electrons population (25% of excited ones) and from the population via r_{ISC} process (the remaining 75% of excited electrons). In the first case, with a very high transition probability k_P , we have a prompt fluorescence (PF) whereas in the second situation, depending on a lower k_{rISC} probability, we have a delayed fluorescence (DF). A strong TADF emission is usually observed in molecules where the yield of triplet levels formation (by intersystem crossing), as well the singlet level formation (by reverse intersystem crossing) are high (particularly the last one as expected). In this condition, we must assume that the r_{ISC} yield that is given by $\phi_{rISC} = \frac{k_{rISC}}{k_{rISC} + k_{nRP} + k_{rP}}$ is approximately equal to 1. This appears when (and usually found in TADF materials) $k_{rISC} \gg k_{nRP} + k_{rP}$, meaning that all relaxation process from triplet excited state are much less probable than the r_{ISC} (as expected). The emission from a TADF material is naturally the sum of the observed from the PF and DF and therefore its quantum yield is given by:

$$\phi_{TADF} = \phi_{PF} + \phi_{DF} = \phi_{PF} \frac{1}{1 - \phi_{rISC} \phi_{ISC}} \quad (5)$$

According [32], if the ratio ϕ_{DF}/ϕ_{PF} is near (or above) four, the yield of the $rISC$ process will be near 100%. In practice, most TADF materials where the value of ΔE_{ST} is less than near 150 mV, such yield is obtained. In this situation, the triplet yield is relatively easy to obtain with precision, and is given by:

$$\phi_{ISC} = \frac{\phi_{DF}}{\phi_{DF} + \phi_{PF}} \quad (6)$$

This relationship can be useful to determine the ratio of ϕ_{DF}/ϕ_{PF} that is a fundamental key for the material characterization. In simple but practical ways, two different approaches can be used for such determination. Both are related to the fact that almost know TADF materials exhibit very poor or none DF in the presence of oxygen. Thus, measuring the luminescence emission parameters under a normal or degassed environment, we can achieve either PF or PF + DF. Under steady state photo physics, the direct measurement of the luminescence spectra in both environment conditions

will give only (with great certainty) the PF (normal environment) and PF + DF (degassed environment). The direct ratio of the integrated spectra (intensity) further gives a very precise value for ϕ_{DF}/ϕ_{PF} . Naturally this simple calculation is possible (quantum yield ratio from integrated intensity) because the intensity is proportional to the quantum yield and, in the case of TADF materials, the values of the proportionality constants for both emissions (DF and PF) are the same due to the fact that both arise from the same excited energy level [33]. The exact calculation is the performed considering the simple relationship is given by $\frac{I_{DF+PF}}{I_{PF}} = \frac{\phi_{DF} + \phi_{PF}}{\phi_{PF}} = 1 + \frac{\phi_{DF}}{\phi_{PF}}$. **Figure 3** shows a simple example of this behavior.

By another hand, the higher transition probability associated with PF compared to the DF probability (that in a crude way depends on the $rISC$ process probability) allows an experimental emission separation under the time-resolved photoluminescence (TRP). In a typical TADF material, the PF lifetime is in the order of dozens of ns whereas the DF lifetime falls into μs . Therefore, measuring both lifetimes, an estimative of the ϕ_{DF}/ϕ_{PF} can be done because the transition probabilities are related to the inverse of the lifetime. If we consider (and is a very good approach) that the emission follows a single exponential decay for both PF and DF, therefore the measured photoluminescence intensity under time can be simply given by the sum of the two single exponential decay expressions as follow:

$$I(t) = I_0^{PF} \exp\left(-\frac{t}{\tau_{PF}}\right) + I_0^{DF} \exp\left(-\frac{t}{\tau_{DF}}\right) \quad (7)$$

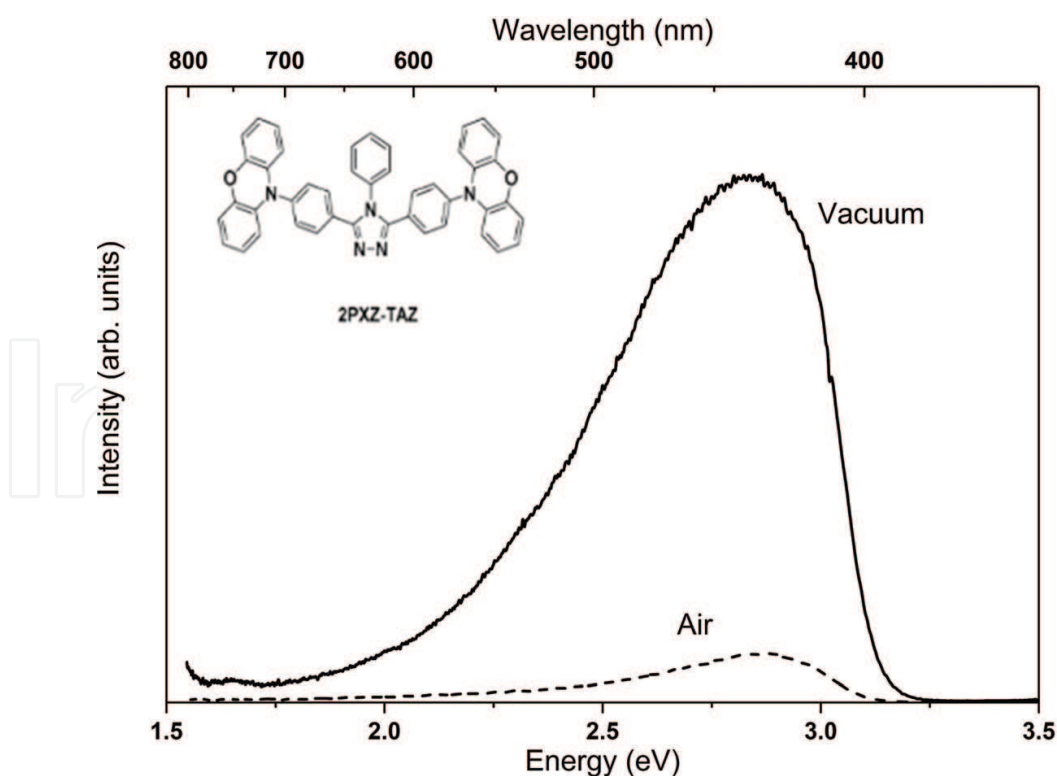


Figure 3. Steady state photoluminescence spectra of 2PXZ-TAZ under normal (air) and degassed (vacuum) environments. The ratio of integrated spectrum in both situations allows a simple calculation of the DF/PF quantum yield. In this case, the ratio ϕ_{DF}/ϕ_{PF} is near 9.

being τ_{PF} , I_0^{PF} , τ_{DF} and I_0^{DF} the lifetime and pre-exponential intensity factor for the PF and DF. Once again, calculating the intensity (integral) for both time-resolved emissions, the ϕ_{DF}/ϕ_{PF} can be obtained and is given simply by:

$$\frac{\phi_{DF}}{\phi_{PF}} = \frac{I_0^{DF} \times \tau_{DF}}{I_0^{PF} \times \tau_{PF}} \quad (8)$$

Finally, and by TRP is possible to estimate the transition probability of the $rISC$ process. Knowing the values for quantum yields and lifetime, an estimation for k_{rISC} can be given by (and considering $\phi_{rISC} \approx 1$)

$$k_{rISC} = \frac{1}{\tau_{DF}} \left(\frac{\phi_{PF} + \phi_{DF}}{\phi_{PF}} \right) \quad (9)$$

Due to several different kinds of triplet harvesting in an organic molecule, sometimes is not simple to attribute an enhanced luminescence to a TADF process. For instance, triplet-triplet annihilation (TTA) is also a wide investigated process for emission efficiency improvement. Distinguish both process is important. Due to the competition between the triplet quenching and decay of triplet states, usually the DF from TTA is non-linear on excitation energy; on the contrary, and because TADF process is purely intramolecular, its DF must follow a linear relationship with excitation energy. **Figure 4** shows an example of the 2PX-TAZ emitter.

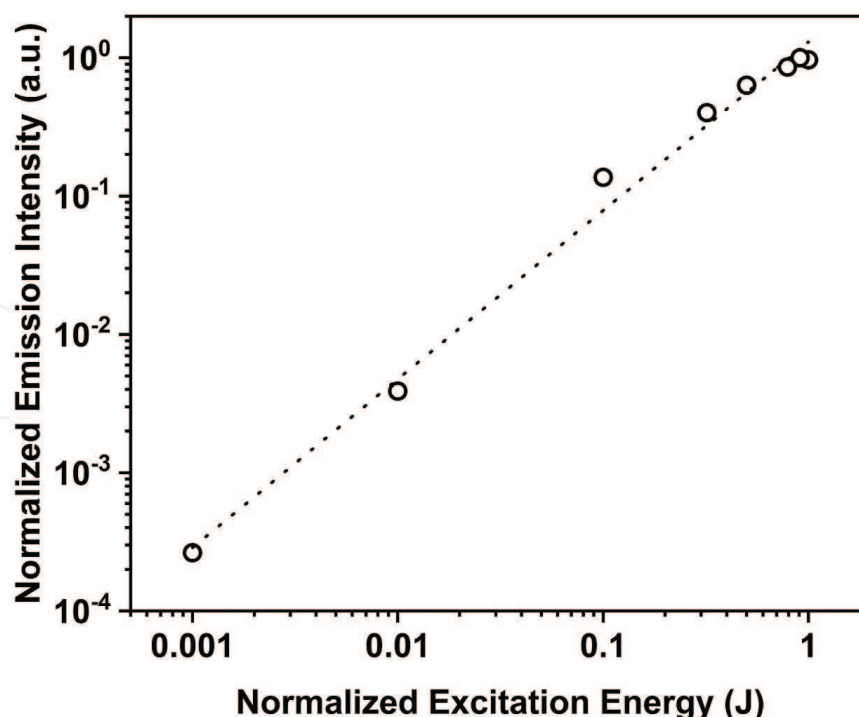


Figure 4. Emission intensity of 2PX-TAZ emitter as a function of excitation energy. The perfect linear fit is the expected result for a TADF material.

Besides the excitation energy dependence, the TADF emission is also strongly dependent on temperature. As the DF is thermally activated, we expect that its intensity decreases strongly with temperature and eventually vanishes at very low temperature. On the contrary, PF must be unaffected by thermal variations. This means that under TRP we must observe a decrease of the high lifetime emission as temperature decreases until remaining only the fast component.

The full understanding of the photo physics properties of the TADF emitter is naturally of extreme importance for further OLED development.

4. OLEDs based on TADF emitters

In the contest of finding best organic emitters for the lightening industry, in 2011 Adachi et al. [34] reported the very first purely organic TADF emitter **PIC-TRZ** (**Figure 5**) which showed promising calculated PLQY in a host matrix of mCP and was 39% and the device showed 5.3% EQE. Since then, in the past 5 years, over 200 new compounds have been reported. Among various emitters, many of them showed EQE of more than 20% composed in a device and this can be reached up to 30% using stipulated device structure with an optimized concentration of TADF emitters and fabrication process [35]. There have been several reviews published focusing on photo physics, device characteristics of TADF and chemistry of TADF emitters [20, 23, 35]. Apart from the use of TADF molecules for OLEDs, there are some challenges must be taken

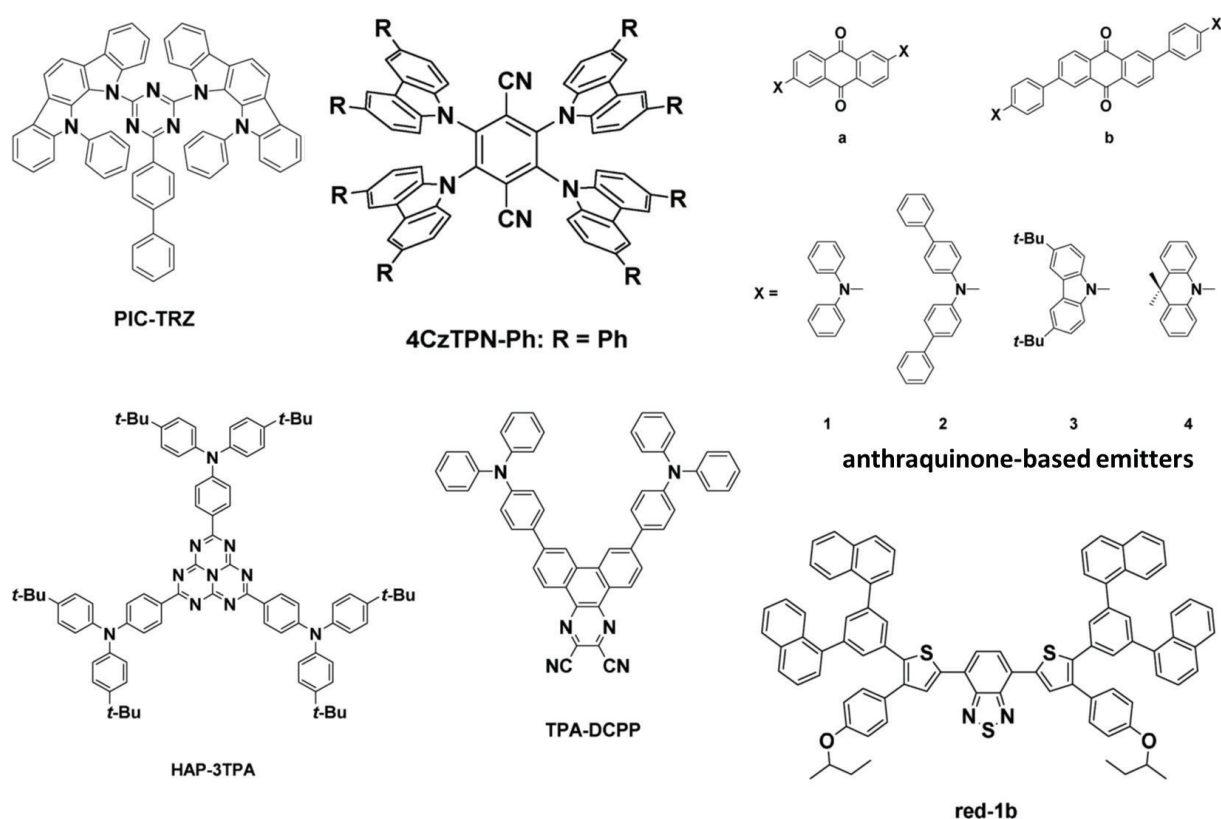


Figure 5. Chemical structures of red-orange TADF emitters.

for the development of TADF emitters such as these emitters are very limited and only few can be used for highly EQE and stable OLEDs, another is the lower maximum brightness and roll-offs at high brightness related triplet annihilation [20, 36]. These can be solved by understanding the structure-property relationship in emitters. In this chapter, we focused more on the photo physical relation of TADF emitter with device performance. In this section, we will describe different TADF emitters and their photo physics-device performance characteristics.

The application of TADF emitters is generally focused on OLEDs applications. As we have discussed in photo physics behavior of TADFs, it requires a solid host to disperse TADF emitters and this host material has a strong influence on the photo physical properties of these emitters [37]. To encounter this, the design and optimization of TADF emitter is a key factor for the fabrication of OLEDs, and this requires the photo physical characterization of TADF in the host molecule which used in the device. Some of the most used hosts are DPEPO, CBP, mCP, mCBP, TPBi, TCTA and TAPC. The OLEDs are usually fabricated by thermally vacuum deposition, but several reports have been focused on fabrication via spin coating solution processed methods which is more suitable for large area OLEDs.

Many groups reported various green TADF based on different donor and acceptor molecules, due to less space it is difficult to discuss all of them. Herein, we will discuss some of the TADF red, green and blue emitters based on their donor and acceptor groups, photo-physical characteristics, and device performance.

4.1. Red-orange TADFs

Herein, we present red-orange TADF emitters which exhibit an electroluminescence peak at wavelength (EL_{max}) > 580 nm. The first reported red TADF emitter, **4CzTPN-Ph** (Figure 5) with green emission by Adachi et al. [38] Figure which exhibits calculated PLQY of 26% in toluene and, τ_d 1.1 μ s. The device showed remarkable EQE of 11.2%, the fabricated device structure was ITO/NPD/5 wt% **4CzTPN-Ph**:CBP/TPBi/LiF/Al. In another report [39], they demonstrated the effect of a higher transition dipole moment which is induced by increasing the distance between D-A units. They compared orange-red anthraquinone based TADFs based on D-A-D (**a1-a4**) and D-Ph-A-Ph-D (**b1-b4**) molecular scaffold showing higher PLQY. The fabricated device was ITO/HAT-CN/Tris-PCz/10wt% **TADF emitter**:CBP/T2T/Bpy-TP2/LiF/Al (Tris-PCz = 9,9'-diphenyl-6-(9-phenyl-9H-carbazol-3-yl)-9H,9'H-3,39'H-bicarbazole; T2T = 2,4,6-tris(biphenyl-3-yl)-1,3,5-triazine; Bpy- TP2 = 2,7-di(2,2'-bipyridin-5-yl)triphenylene) using **b1** emitter. The compound showed 80% PLQY and τ_d 416 μ s in a host CBP matrix. The calculated ΔE_{ST} from experimental value was 0.24 eV. The device exhibit 12.5% EQE and the CIE coordinates were (0.61, 0.39).

In 2013, Li et al. [40] synthesized orange-red emitter, **HAP-3TPA** (Figure 5), based on heptazaphenalene acceptor with a small ΔE_{ST} of 0.17 eV ΔE_{ST} of 0.17 eV. The molecules show absorbance at 610 nm. The calculated PLQY of 6 wt% TADF in a host matrix 26mCPy was 91%, and the τ_d of 100 μ s. The molecule showed very weak TADF behavior, and the ϕ_{DF}/ϕ_{PF} was 0.07 compared to ϕ_{DF}/ϕ_{PF} of 1.58 in the fabricated device i.e. ITO/NPD/6 wt% **HAP-3TPA**:26mCPy/Bphen/Mg:Ag/Ag with a high EQE value of 17.5% and the CIE was (0.60, 0.40).

In another study, Wang et al. [41] demonstrated the effect of the twist angle during the designing strategy of TADF emitters. This twist angle can be reduced by increasing the D-A distance which gives an orbital overlap to increase k_t . They synthesized the first near-infrared (NIR) TADF emitter **TPA-DCPP** (**Figure 5**) based on dicyanodiazatriphenylene acceptor moiety. The experimental calculated ΔE_{ST} was 0.13 eV. The calculated PLQY of 10 wt% **TPA-DCPP** in TPBi host matrix was 50%, and the τ_d of 86.2 μ s. The fabricated device ITO/NPB/TCTA/20 wt% **TPA-DCPP**:TPBi/TPBi/LiF/Al exhibit EQE value of 9.8% with the CIE at (0.68, 0.32). Similarly, Chen et al. [42] also reported a novel solution processed red TADF using **red-1b** molecule which can undergo both TADF and TTA process, depends on current density. The calculated ΔE_{ST} was 0.40 eV. The photo-physical characteristics of the molecule are λ_{max} of 622 nm and the solid state calculated PLQY of 28%, while the EQE was very low 1.75% in fabricated device. Very recently in another report, Data et al. [43] reported dibenzene-phenazine acceptors based TADF emitters which showed a formation of exciplex when doped in m-MTDATA host and a strong NIR emission at 741 nm was observed with EQE of 5%, but no concluded evidence was provided in the work to support the TADF mechanism of this exciplex system.

4.2. Blue TADF emitters

In 2012, Adachi et al. reported the very first class of blue TADF emitter based on diphenylsulfone (**DPS**) as an acceptor [27] (see **Figure 6**).

To synthesize efficient blue TADF emitter and their use in the device, it is important to take account of the π -conjugation length and the redox potential of the donor and acceptor moieties and in DPS derivatives the advantage is that the oxygens of the sulfonyl group have significant electronegativity, which gives the sulfonyl group electron-withdrawing properties and sulfonyl group exhibit tetrahedral geometry which limit the conjugation [35]. The device fabricated with 10 wt% emitter showed good results, the device ITO/ α -NPD/TCTA/CzSi/10 wt% *TADF emitter*:DPEPO/ DPEPO/TPBi/LiF/Al and the EQE was 9.9%, the emitter incorporated in the device was **DTS-DPS** [44]. The photo-physical characteristics of the molecules are λ_{max} of 423 nm. The calculated PLQY in DPEPO host was 80% and τ_d was to be 540 μ s. The ΔE_{ST} was 0.32 eV. They suggested that for small ΔE_{ST} , the energy gap between 3LE and 3CT must be small, and the *r*IC occurs from 3LE to 3CT which was followed by *r*ISC to 1CT and similar results were seen in other derivatives. In a similar approach, Dias et al. proposed a mechanism to understand the mechanism of *r*ISC in such type of molecules [45]. The results suggested that *r*ISC mechanism is still possible if the ΔE_{ST} is greater than 0.3 eV. They studied a molecule DTC-DBT (**Figure 6**), where the ΔE_{ST} is 0.35 eV, but in the molecule, it is possible to harvest 100% triplet excitons. According to the authors, the presence of heteroatom lone pairs form "hidden" $3n-\pi^*$ state sandwiched between higher 3CT and lower 3LE states and the up-conversion follow the pattern: $^3LE \rightarrow -3n-\pi^* \rightarrow ^3CT \rightarrow ^1CT$. In similar study, Chen et al. [46] demonstrated the importance of "non-adiabatic effects in butterfly donor-acceptor-donor molecules" **DTC-DBT**, and suggested that upon the rotation of D-A groups, a conical intersection (C_1) between long-lying excited states and at C_1 "the non-adiabatic coupling matrix element between two excited states becomes infinite, which is proportional to the RISC rate." This was further supported by Etherington et al. [47].

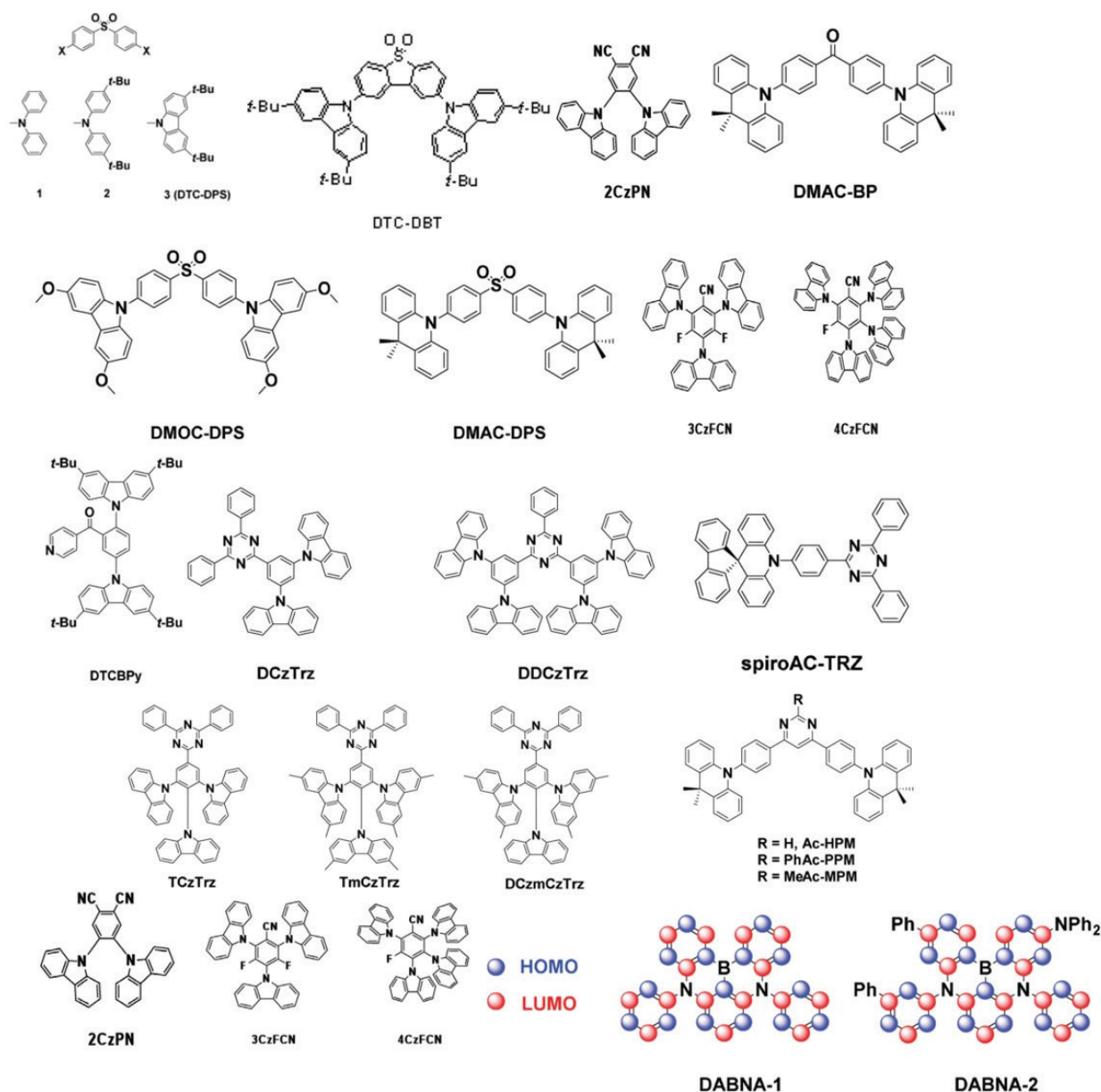


Figure 6. Chemical structures of blue TADF emitters.

Adachi et al. [48] reported deep blue emitters **DMOC-DPS** (Figure 6) with the ΔE_{ST} of 0.21 eV. The calculated PLQY in DPEPO host at 10 wt% was 80% along with measured τ_d of 114 μ s and the device ITO/a-NPD (30 nm)/TCTA (20 nm)/CzSi (10 nm)/ **DMOC-DPS**:DPEPO (20 nm)/ DPEPO (10 nm)/TPBI (30 nm)/LiF (0.5 nm)/Al showed an EQE of 14.5%. They further reported another blue TADF **DMAC-DPS** with the absorbance of 464 nm. The PLQY in mCP host was 80%, and τ_d was 3.1 μ s. For this **DMAC-DPS**, the experimentally calculated ΔE_s was very low and was 0.08 eV. The fabricated device performed at an excellent EQE of 19.5% [44], where the reduced ΔE_{ST} is a result of higher 3LE state than 3CT state, caused by inducement of dimethylacridan donor. Another molecule **DMAC-BP** which ΔE_{ST} is 0.07 eV with calculated PLQY of 85%, and τ_d of 2.7 μ s showed EQE of 18.9%.

It is very important to design the geometry of TADF molecule to induce TADF process, to counter this, Rajmalli et al. [49] reported novel blue TADF emitters based on benzoylpyridine acceptor **DCBPy** and **DTCBPy**, in **DTCBPy** (Figure 6) a tert-butyl group is present. Upon photo-physical characterization, the second molecule **DTCBPy** showed a small redshift in emission by 4 nm. The ΔE_{ST} was smaller in both emitters, and was 0.07 and 0.08 eV in **DCBPy** and **DTCBPy**, respectively. The calculated PLQY in host matrix was 88 for **DCBPy** and 91% for **DTCBPy**. The PLQY in the solid state was 91% compared to lower 14–36% in solution. The device exhibit sky-blue and green emission. The EQEs was 24.0% CIE (0.17, 0.36) and 27.2% CIE (0.30, 0.64) for **DCBPy** and **DTCBPy**, respectively. The efficiency roll-off was low at practical brightness level.

In 2015, Kim et al. [50] synthesized two new blue TADF emitters **DCzTrz** and **DDCzTrz** (Figure 6), where “two additional carbazole moieties attached to phenyl ring in a meta fashion” in **DDCzTrz** and as “meta linkage” both emitters have similar emission as well as ΔE_{ST} . The photo-physical characteristics of both molecules are absorbance maximum of 420 and 430 nm. The calculated PLQY for both emitters was 43 and 66%, respectively. The smaller ΔE_{ST} 0.25 eV for **DCzTrz** and 0.27 eV for **DDCzTrz**. The OLED using **DDCzTrz** showed an excellent EQE of 18.9% but in the device, the LT80 (time required to drop 80% luminescence) was 52 h, three-time longer than conventional blue phosphorescent Iridium complex. It is due to first stabilization through carbazole moiety, secondly, stable positive carbazole and negative triazine excited state pair, and thirdly excellent glass transition temperature for both 160 for **DCzTrz** and 218°C for **DDCzTrz** give the stability to the device. But the device composed of **DCzTrz** was stable only for 5 h and this caused due to the high emission of the molecule. Upon modification of **DCTrz** through the addition of more carbazole donors, they synthesized another three molecules **TCzTrz**, **TmCzTrz**, and **DCzmCzTrz** (Figure 6). Where calculated PLQY was 100% in DPEPO host, and the ΔE_{ST} was 0.16, 0.07, and 0.20 eV, respectively [51]. It was found that in **TCzTrz** the ΔE_{ST} is lower by 0.09 eV compare to **DCzTrz**. The device composed of **TCzTrz** showed an excellent EQE of 25.5%, while **TmCzTrz** and **DCzmCzTrz** showed EQE of 25.3 and 21.3%, respectively.

In another study, Lin et al. demonstrated [52] a novel triazine-based blue TADF emitter named **spiroAC-TRZ** (Figure 6) which showed photo-physical characteristics of calculated PLQY of 100% in 12 wt% mCPCN host, τ_d of 2.1 μ s. The experimentally calculated ΔE_{ST} was very small and to be 0.07 eV. The device ITO/ MoO₃/TAPC/mCP/12 wt% **spiroAC-TRZ**:mCPCN/3TPYMB/ LiF/Al an EQE of 37%, which is highest among the reported blue TADF. In a similar approach, Komatsu et al. [53] reported three novel deep blue TADF (Figure 6). **Ac-RPMs**, on the modification of triazine acceptor to pyrimidine. All the compounds exhibited similar photo-physical properties i.e. PLQY of 80%, τ_d of 26.2 μ s in a host matrix at 10 wt% in DPEPO and the calculated ΔE_{ST} was 0.19 eV for **Ac-MPM**, and the OLEDs showed an EQE of 24.5% and CIE coordinates of (0.19, 0.37), interestingly the turn-on voltage was very low and was 2.80 V, such device can be used for highly efficient light devices.

Among various D-A and D-A-D structured TADF molecules, the main chemical moiety plays an important role for the exhibition of the TADF behavior, and as we have discussed various acceptors have been used for the synthesis of TADF materials, among them Cyano-based

acceptors are used as most usual building blocks for the synthesis of deep-blue TADF. The first Cyano based blue TADF **2CzPN** (**Figure 6**) was firstly reported by Adachi et al. [36] PLQY of 47% in solution state and the EQE was 13.6% in device. Sun et al. [54] reported a blue TADF emitter showing an excellent EQE of 21.8% in composed OLED structure of ITO/4 wt% ReO₃:mCP/5 wt% **TADF emitter**:mCP:PO15/4 wt% Rb₂CO₃:PO-15/Al (PO-15 = poly[N,N'-bis(4-butylphenyl)-N,N'-bisphenylbenzidine]) by using a mixed co-host system (mCP:PO15 = 1:1).

Solution-processed TADF materials was reported by Cho et al. [55], they synthesized two blue TADF emitters named **3CzFCN** and **4CzFCN** (**Figure 6**), showing photo-physical characteristics of calculated PLQY in 10 wt% diphenyldi(4-(9-carbazolyl)phenyl)silane (SiCz) host at 10 wt%, and was 74% for **3CzFCN** and 100% for **4CzFCN**, while the experimentally calculated small ΔE_{ST} of 0.06 eV for both emitters. The λ_{max} was 440 and 460 nm, respectively. The fabricated device with **4CzFCN** emitter showed an excellent EQE of 20% with CIE coordinates of (0.16, 0.26), the device structure was ITO/PEDOT:PSS/PVK/15 wt%**4CzFCN**:SiCz/TPBI/LiF/Al.

In another study, very recently, Hatakeyama et al. [56] demonstrated synthesis of boron-based acceptor TADFs. They synthesized TADF emitters **DABNA-1** and **DABNA-2** (**Figure 6**) showing ΔE_{ST} of 0.18 and 0.14 eV, respectively. The λ_{max} was 460 and 469 nm, while calculated PLQY in mCBP host at 1 wt% was 88 and 90%. The device fabricated with **DABNA-2** emitter showed an excellent EQE of 20.2%. In such boron based TADFs, the ΔE_{ST} is very low, this is due to the presence of strong LUMO localization called as “multiple resonance effect”, induced by boron atom. The PLQY in solid state is 87–100%, which makes boron based TADF emitter a potential candidate for blue TADFs.

4.3. Green-yellow TADFs

Among various TADF emitters, plenty of them are the green-yellow emitter and most those green to yellow emitters are based on cyano-based acceptors. The molecular design of these cyano-based emitters is based “on the presence of a twisted conformation of donor carbazoles with respect to phthalonitrile plane” to confer the HOMO-LUMO separation and result to lower ΔE_{ST} . These cyano-based green TADF emitters are classified in three categories: (a) monomeric series with orthosteric hindrance, (b) homoconjugation series, and (3) dimeric emitters. In monomeric emitters, ΔE_{ST} is very small and high PLQY yield. In homoconjugation series, the HOMO and LUMO separation is easily achievable but lower PLQY yield and in dimeric series the ΔE_{ST} is very higher i.e. 0.11–0.21 eV. The first green emitter was reported by Adachi et al. [38] in 2012, **4CzIPN** (**Figure 7**), exhibiting ΔE_{ST} of 0.08 eV. The calculated PLQY in CBP host was 82% and τ_d of 3370 μ s and the device showed excellent 19.3% EQE.

In the similar contest, Taneda and co-workers [57] synthesized a highly efficient green TADF emitter **3DPA3CN** (**Figure 7**) and it showed PLQY of 100% in solid state and 100% triplet harvesting via *rISC* mechanism. The molecule showed photo-physical characteristics of absorbance of 533 nm. The calculated PLQY of 6 wt% thin film in DPEPO host matrix was 100% while the τ_d was 550. The ΔE_{ST} was to be small 0.10 eV and is due to the strongly localized molecular geometry the HOMO and LUMO, which gives the small separation between

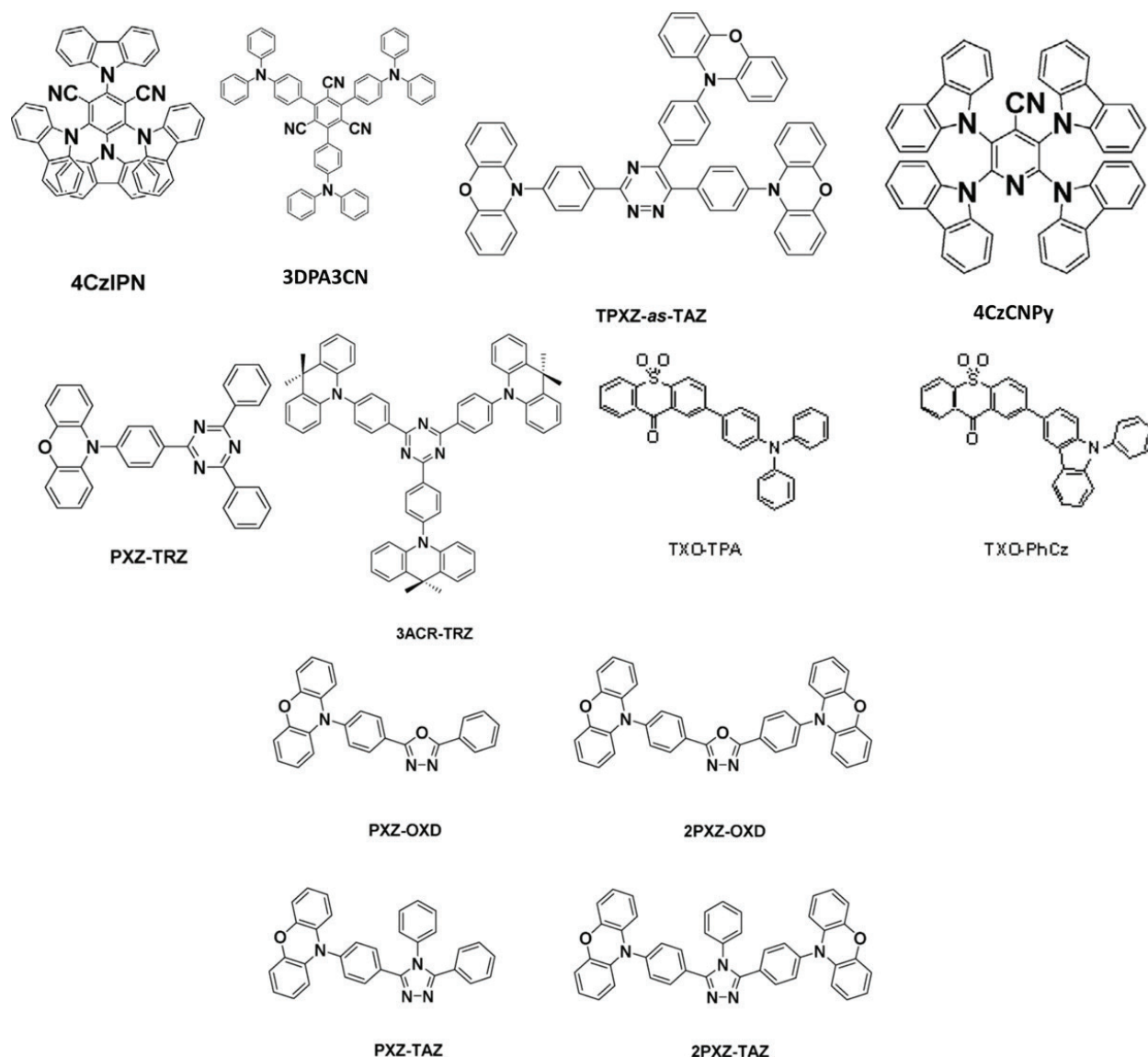


Figure 7. Chemical structures of green-yellow TADF emitters.

HOMO and LUMO. The fabricated device ITO/ α -NPD/mCBP/6 wt% *TADF emitter*:DPEPO/TPBI/LiF/Al) shows an excellent EQE of 21.4% with EL_{\max} at ≈ 540 nm. In another study, Xiang et al. [58] reported a triazine based acceptor along with phenoxazine as donor and synthesized a yellow TADF emitter **TPXZ-as-TAZ** (**Figure 7**) with very low ΔE_{ST} of 0.03 eV. The molecule showed excellent EQE of 13%. The calculated PLQY in 1.5 wt% thin film in host CBP was 53% while the calculated τ_d was to be 1.10 μ s. The λ_{\max} for emitter was 555 nm.

Tang et al. revealed the strategy to synthesized solution processed green TADF emitters [59]. They synthesized emitter **4CzCNPy** (**Figure 7**) which has small ΔE_{ST} of 0.07 eV. The λ_{\max} for emitter was 560 nm. The calculated PLQY was quite low in toluene with a value of 55% and τ_d calculated of 8.4 μ s. The fabricated device ITO/PEDOT:PSS/8 wt% *TADF emitter*:mCP/TmPyPB/LiF/Al showed EQE of 11.3% and CIE coordinate was (0.34, 0.59). They suggested that without cyano group the TADF emission could not be observed in the molecule along

with enhancement to the PLQY. In this molecule, the emission is dominated by ^1CT state to reduce the $n\text{-}\pi^*$ quenching of the 4CzPy group.

Apart from Cyano-based green TADF emitters, many researchers reported TADF emitters based on 1,2,5-triazine acceptor (**TRZ**). Tanaka and co-workers [60] reported in 2012 a TADF emitter **PXZ-TRZ** (**Figure 7**) with a small ΔE_{ST} exhibiting λ_{max} : near 540 nm. The calculated PLQY of the thin film in 6 wt% CBP was 66%, while τ_d was 0.68 μs . The twisted structure of the phenoxazine can easily be achieved and induces the charge transfer, results to a small ΔE_{ST} of 0.07 eV. In such molecule, the dihedral angle between donor and acceptor is 74.9, which helps to localize the HOMO and LUMO for efficient TADF exhibition. The device was fabricated using the emitter ITO/ α -NPD/6 wt% *TADF emitter*:CBP/TPBi/LiF/Al showed EQE of 12.5%. Adachi et al. [61] also reported another green emitter based on TRZ acceptor, **3ACR-TRZ** (**Figure 7**), with a small ΔE_{ST} of 0.02 eV which can be solution processed. It exhibits the Photo-physical characteristics of λ_{max} of 504 nm. The calculated PLQY in 16 wt% CBP was near a unit value of 98% and τ_d of 6.7 μs in Host matrix, while in device ITO/PEDOT:PSS/16 wt% *TADF emitter*:CBP/BmPyPhB/Liq/Al, the EQE was 18.6% along with EL_{max} at 520 nm.

In 2014, Wang et al. reported [62] sulfone-based acceptor green TADF emitters. They synthesized two green TADF emitter named **TXO-PhCz** and **TXO-TPA** (**Figure 7**). The photo-physical characteristic of these molecules is λ_{max} of 520 nm, calculated PLQY of thin film was 90% in 5 wt% mCP, and a small ΔE_{ST} value of 0.07 eV for TXO-PhCz and λ_{max} of 580 nm, the PLQY of thin film was 83% and even smaller ΔE_{ST} of 0.05 eV were demonstrated. The fabricated device structure was ITO/PEDOT (30 nm)/TAPC (20 nm)/*TADF emitter* 5 wt%: mCP (35 nm)/TmPyPB (55 nm)/LiF(0.9 nm)/Al and the device showed an EQEs of 21.5% for **TXO-TPA** emitter and 18.5% for **TXP-PhCz** emitter, respectively with the turn-on voltage of 4.7–5.2 V which is low for such devices.

1,3,4-Oxadiazole was used to synthesized green TADF emitter and these emitters are most commonly used for the applications. Three new green TADF emitters were synthesized by Lee et al. [63]. The three emitters were **PXZ-OXD**, **PXZ-TAZ**, **2PXZ-OXD**, and **2PXZ-TAZ** (**Figure 7**). In emitters, the D-A moieties, where the donor was phenoxazine group while the acceptor was 1,3,4-oxadiazole and 1,2,4-triazole. In molecules, the PLQY was calculated in a host material and the PLQY was high in donor-acceptor-donor **2PXZ-OXD** and **2PXZ-TAZ** with high $r\text{ISC}$ compare to donor-acceptor **PXZ-OXD** and **PXZ-TAZ** molecules. The best device showed an EQE of 14.9% with emitter as **2PXZ-OXD**. The emitter exhibit photo-physical characteristics of λ_{max} of 517 nm, PLQY yield was 87%, τ_d of 520 μs in 6 wt% DPEPO and the ΔE_{ST} of 0.15 eV and the fabricated device structure was ITO/NPD (30 nm)/mCP (10 nm)/6 wt% *TADF emitter*: DPEPO (15 nm)/DPEPO (10 nm)/TPBi (40 nm)/ LiF (0.8 nm)/Al (90 nm).

Many groups reported various green TADF based on different donor and acceptor molecules. The more significant are focused here.

5. Conclusions and outlook

Past few years have witnessed tremendous development in the field of organic electronics and especially in synthesis of organic light emitting materials which helped to boost the cost

reduction of OLEDs and performance enhancement. The potential inexpensive synthesis methods, OLEDs fabrication process, flexibility and lightweight make them one of the promising materials for energy devices. A large number of phosphorescent and fluorescent organic materials have been already synthesized for their use in OLEDs. Recently, TADF materials have been introduced in OLEDs fabrication to achieve 100% IQE and high EQE, which can be achieved near 50%.

The actual development of organic TADF emitters achieves a status that surpasses a simple curiosity. The new OLED framework based on highly efficient TADF materials opens a new field of applications for display and lightening. These materials, based on separated donor-acceptor moieties in one molecule, leads to a unique luminescent process of a triplet harvesting in the excited state with a further huge increase of internal efficiency up to the 100% limit. This simple way to tailored pure organic emitters is really one of the most recent advances in chemistry and OLEDs filed. Achieving very high external efficiencies without using an expensive and rare transition metals, puts the organic emitters towards new possibilities. Particularly important is the application in lighting from large area emitters, a field that is until now, a technological problem. The possibility to have a full range color emitters with high efficiency (as shown, and particularly in blue) is also an outstanding achievement towards a new device design and application, particularly in white emission. Nevertheless, improving the efficiency towards the theoretical efficiency limit, can only be achieved with a deep understand of the TADF process in these organic molecules. This is due to the fact that the interactions between energy levels of TADF emitter and the host can condition the emission due to the TADF process itself as referred before. Thus, the next steps must be focused on the physical models for this *rISC* pathway and the relationship with the molecular structure. In the OLEDs point of view, the design of reliable host materials that fulfills the requirements needs to allow an efficient luminesce emission form the TADFs. A new era is opened.

TADFs have been studied and used for OLEDs so far, and this field is relatively young but it has developed significantly during the past 5 years. By the incorporation of TADFs 40–50% EQE can be achieved. However, at the present stage despite of numerous characterization techniques to understand the TADF behavior, more rigorous efforts are required for their understanding and use for commercially production. The fabrication cost of the OLEDs based on TADF emitter should be less to make them major candidate in both display and lightening industry and the cost is critical. To reduce the cost, it is necessary to develop solution processed OLED fabrication methods and synthesis of polymeric or dendrimeric TADF emitters. These TADFs have already been found a significant role in next-generation displays and lightning materials and their use can only be realized as their synthesis characterization and device fabrication progresses.

Acknowledgements

The authors would like to acknowledge the i3N support from UID/CTM/50025/2013 and the EXCILIGHT Project from the European Union's Horizon 2020 research and innovation program under the Marie Skłodowska-Curie grant agreement No 674990.

Author details

Manish Kumar^{1,2}, Miguel Ribeiro¹ and Luiz Pereira^{2*}

*Address all correspondence to: luiz@ua.pt

1 CeNTI – Centre for Nanotechnologies and Smart Materials, R. Fernando Mesquita, Portugal

2 Department of Physics and i3N – Institute for Nanostructures, Nanomodulation and Nanofabrication, University of Aveiro, Portugal

References

- [1] Tang CW, Van Slyke SA. Organic electroluminescent diodes. *Applied Physics Letters*. 1987;**51**(12):913-915. DOI: 0.1063/1.98799
- [2] Yersin H. *Highly Efficient OLEDs with Phosphorescent Materials*. 1st ed. Verlag GmbH & Co. KGraA: Wiley-VCH; 2008
- [3] Franky S, editor. *Organic Electronics Materials, Processing, Devices and Applications*. 1st ed. Boca Raton: CRC Press; 2010
- [4] Gaspar DJ, Polikarpov E, editors. *OLED Fundamentals: Materials, Devices, and Processing of Organic Light-Emitting Diodes*. 1st ed. Boca Raton: CRC Press; 2015
- [5] Sasabe H, Kido J. Recent progress in phosphorescent organic light-emitting devices. *European Journal of Organic Chemistry*. 2013;**2013**(14):7653-7663. DOI: 10.1002/ejoc.201300544
- [6] Baldo M, Lamansky S, Burrows P, Thompson M, Forrest S. Very high-efficiency green organic light-emitting devices based on electrophosphorescence. *Applied Physics Letters*. 1999;**75**(1):4-6. DOI: 10.1063/1.124258
- [7] Adachi C, Baldo MA, Thompson ME, Forrest SR. Nearly 100% internal phosphorescence efficiency in an organic light-emitting device. *Journal of Applied Physics*. 2001;**90**(10):5048-5051. DOI: 10.1063/1.1409582
- [8] Tsuzuki T, Nakayama Y, Nakamura J, Iwata T, Tokito S. Efficient organic light-emitting devices using an iridium complex as a phosphorescent host and a platinum complex as a red phosphorescent guest. *Applied Physics Letters*. 2006;**88**(24):243511. DOI: 10.1063/1.2213017
- [9] Kwong RC, Sibley S, Dubovoy T, Baldo M, Forrest SR, Thompson ME. Efficient, saturated red organic light emitting devices based on phosphorescent platinum(II) porphyrins. *Chemistry of Materials*. 1999;**11**(12):3709-3713. DOI: 10.1021/cm9906248
- [10] Kalinowski J, Fattori V, Cocchi M, Williams JG. Light-emitting devices based on organometallic platinum complexes as emitters. *Coordination Chemistry Reviews*. 2011;**255**(21):2401-2425. DOI: 10.1016/j.ccr.2011.01.049

- [11] Sun Y, Giebink NC, Kanno H, Ma B, Thompson ME, Forrest SR. Management of singlet and triplet excitons for efficient white organic light-emitting devices. *Nature*. 2006; **440**(7086):908-912. DOI: 10.1038/nature04645
- [12] Tanaka D, Sasabe H, Li YJ, Su SJ, Takeda T, Kido J. Ultra high efficiency green organic light-emitting devices. *Japanese Journal of Applied Physics*. 2006; **46**(1L):L10. DOI: 10.1143/JJAP.46.L10
- [13] Reineke S, Lindner F, Schwartz G, Seidler N, Walzer K, Lüssem B, Leo K. White organic light-emitting diodes with fluorescent tube efficiency. *Nature*. 2009; **459**(7244):234-238. DOI: 10.1038/nature08003
- [14] Helander MG, Wang ZB, Qiu J, Greiner MT, Puzzo DP, Liu ZW, Lu ZH. Chlorinated indium tin oxide electrodes with high work function for organic device compatibility. *Science*. 2011; **332**(6032):944-947. DOI: 10.1126/science.1202992
- [15] Tao Y, Wang Q, Yang C, Zhong C, Qin J, Ma D. Multifunctional triphenylamine/oxadiazole hybrid as host and exciton-blocking material: High efficiency green phosphorescent OLEDs using easily available and common materials. *Advanced Functional Materials*. 2010; **20**(17):2923-2929. DOI: 10.1002/adfm.201000669
- [16] Lee CW, Lee JY. Above 30% external quantum efficiency in blue phosphorescent organic light-emitting diodes using Pyrido [2, 3-b] indole derivatives as host materials. *Advanced Materials*. 2013; **25**(38):5450-5454. DOI: 10.1002/adma.201301091
- [17] Baldo MA, O'Brien DF, You Y, Shoustikov A, Sibley S, Thompson ME, Forrest SR. Highly efficient phosphorescent emission from organic electroluminescent devices. *Nature*. 1998; **395**(6698):151-154. DOI: 10.1038/25954
- [18] Kondakov DY, Pawlik TD, Hatwar TK, Spindler JP. Triplet annihilation exceeding spin statistical limit in highly efficient fluorescent organic light-emitting diodes. *Journal of Applied Physics*. 2009; **106**(12):124510. DOI: 10.1063/1.3273407
- [19] Endo A, Sato K, Yoshimura K, Kai T, Kawada A, Miyazaki H, Adachi C. Efficient up-conversion of triplet excitons into a singlet state and its application for organic light emitting diodes. *Applied Physics Letters*. 2011; **98**(8):42. DOI: 10.1063/1.3558906
- [20] Tao Y, Yuan K, Chen T, Xu P, Li H, Chen R, Zheng C, Zhang L, Huang W. Thermally activated delayed fluorescence materials towards the breakthrough of organoelectronics. *Advanced Materials*. 2014; **26**(47):7931-7958. DOI: 10.1002/adma.201402532
- [21] Adachi C. Third-generation organic electroluminescence materials. *Japanese Journal of Applied Physics*. 2014; **53**(6):060101. DOI: 10.7567/jjap.53.060101
- [22] Pereira L. Organic Light Emitting Diodes - The Use of Rare Earth and Transition Metals. Singapore: Pan Stanford Publishing; 2012. 348p. ISBN: 978-9814267298
- [23] Dias Fernando B, Penfold Thomas J, Monkman AP. Photophysics of thermally activated delayed fluorescence molecules. *Methods and Applications in Fluorescence*. 2017; **5**:012001. DOI: 10.1088/2050-6120/aa537e

- [24] Turro NJ, Scaiano JC, Ramamurty V. Principles of Molecular Photochemistry: An Introduction. 1st ed. Mill Valleri, CA, USA: University Science Books; 2010
- [25] Wong Michael Y, Eli Z-C. Purely organic thermally activated delayed fluorescence materials for organic light-emitting diodes. *Advanced Materials*. 2017;**29**:1605444. DOI: 10.1002/adma.201605444
- [26] Milián-Medina B, Gierschner J. Computational design of low singlet–triplet gap all-organic molecules for OLED application. *Organic Electronics*. 2012;**13**(6):985-991. DOI: 10.1016/j.orgel.2012.02.010
- [27] Zhang Q, Li J, Shizu K, Huang S, Hirata S, Miyazaki H, Adachi C. Design of efficient thermally activated delayed fluorescence materials for pure blue organic light emitting diodes. *Journal of the American Chemical Society*. 2012;**134**(36):14706-14709. DOI: 10.1021/ja306538w
- [28] Lim BT, Okajima S, Chandra AK, Lim EC. Radiationless transitions in electron donor-acceptor complexes: Selection rules for $S_1 \rightarrow T$ intersystem crossing and efficiency of $S_1 \rightarrow S_0$ internal conversion. *Chemical Physics Letters*. 1981;**79**(1):22-27. DOI: 10.1016/0009-2614(81)85280-3
- [29] Nobuyasu RS, Ren Z, Griffiths GC, Batsanov AS, Data P, Yan S, Monkman AP, Bryce MR, Dias FB. Rational design of TADF polymers using a donor–acceptor monomer with enhanced TADF efficiency induced by the energy alignment of charge transfer and local triplet excited states. *Advanced Optical Materials*. 2016;**4**(4):597-607. DOI: 10.1002/adom.201500689
- [30] Ogiwara T, Wakikawa Y, Ikoma T. Mechanism of intersystem crossing of thermally activated delayed fluorescence molecules. *The Journal of Physical Chemistry. A*. 2015;**119**(14): 3415-3418. DOI: 10.1021/acs.jpca.5b02253
- [31] Gibson J, Monkman AP, Penfold TJ. The importance of vibronic coupling for efficient reverse intersystem crossing in thermally activated delayed fluorescence molecules. *ChemPhysChem*. 2016;**17**(19):2956-2961. DOI: 10.1002/cphc.201600662
- [32] Meches G, Goushi K, Potscavage WJ, Adachi C. Influence of host matrix on thermally-activated delayed fluorescence: Effects on emission lifetime, photoluminescence quantum yield, and device performance. *Organic Electronics*. 2014;**15**(9):2027-2037. DOI: 10.1016/j.orgel.2014.05.027
- [33] Dias FB, Santos J, Graves DR, Data P, Nobuyasu RS, Fox MA, Batsanov AS, Palmeira T, Berberan-Santos MN, Bryce MR, Monkman AP. The role of local triplet excited states and D-A relative orientation in thermally activated delayed fluorescence: Photophysics and devices. *Advancement of Science*. 2016;**3**(12):1600080. DOI: 10.1002/advs.201600080
- [34] Kaji H, Suzuki H, Fukushima T, Shizu K, Suzuki K, Kubo S, Komino T, Oiwa H, Suzuki F, Wakamiya A, Murata Y. Purely organic electroluminescent material realizing 100% conversion from electricity to light. *Nature Communications*. 2015;**19**(6):8476. DOI: 10.1038/ncomms9476

- [35] Yang Z, Mao Z, Xie Z, Zhang Y, Liu S, Zhao J, Xu J, Chi Z, Aldred MP. Recent advances in organic thermally activated delayed fluorescence materials. *Chemical Society Reviews*. 2017;**46**(3):915-1016. DOI: 10.1039/C6CS00368K
- [36] Masui K, Nakanotani H, Adachi C. Analysis of exciton annihilation in high-efficiency sky-blue organic light-emitting diodes with thermally activated delayed fluorescence. *Organic Electronics*. 2013;**14**(11):2721-2726. DOI: 10.1016/j.orgel.2013.07.010
- [37] Komino T, Nomura H, Koyanagi T, Adachi C. Suppression of efficiency roll-off characteristics in thermally activated delayed fluorescence based organic light-emitting diodes using randomly oriented host molecules. *Chemistry of Materials*. 2013;**25**(15):3038-3047. DOI: 10.1021/cm4011597
- [38] Uoyama H, Goushi K, Shizu K, Nomura H, Adachi C. Highly efficient organic light-emitting diodes from delayed fluorescence. *Nature*. 2012;**492**(7428):234-238. DOI: 10.1038/nature11687
- [39] Zhang Q, Kuwabara H, Potscavage WJ Jr, Huang S, Hatae Y, Shibata T, Adachi C. Anthraquinone-based intramolecular charge-transfer compounds: Computational molecular design, thermally activated delayed fluorescence, and highly efficient red electroluminescence. *Journal of the American Chemical Society*. 2014;**136**(52):18070-18081. DOI: 10.1021/ja510144h
- [40] Li J, Nakagawa T, Macdonald J, Zhang Q, Nomura H, Miyazaki H, Adachi C. Highly efficient organic light-emitting diode based on a hidden thermally activated delayed fluorescence channel in a heptazine derivative. *Advanced Materials*. 2013;**25**(24):3319-3323. DOI: 10.1002/adma.201300575
- [41] Wang S, Yan X, Cheng Z, Zhang H, Liu Y, Wang Y. Highly efficient near-infrared delayed fluorescence organic light emitting diodes using a phenanthrene-based charge-transfer compound. *Angewandte Chemie, International Edition*. 2015;**54**(44):13068-13072. DOI: 10.1002/anie.201506687
- [42] Chen P, Wang LP, Tan WY, Peng QM, Zhang ST, Zhu XH, Li F. Delayed fluorescence in a solution-processable pure red molecular organic emitter based on dithienylbenzothiadiazole: A joint optical, electroluminescence, and magnetoelectroluminescence study. *ACS Applied Materials & Interfaces*. 2015;**7**(4):2972-2978. DOI: 10.1021/am508574m
- [43] Data P, Pander P, Okazaki M, Takeda Y, Minakata S, Monkman AP. Dibenzo [a, j] phenazine-cored donor-acceptor-donor compounds as green-to-red/NIR thermally activated delayed fluorescence organic light emitters. *Angewandte Chemie, International Edition*. 2016;**55**(19):5739-5744. DOI: 10.1002/anie.201600113
- [44] Zhang Q, Li B, Huang S, Nomura H, Tanaka H, Adachi C. Efficient blue organic light-emitting diodes employing thermally activated delayed fluorescence. *Nature Photonics*. 2014;**8**(4):326-332. DOI: 10.1038/nphoton.2014.12
- [45] Dias FB, Bourdakos KN, Jankus V, Moss KC, Kamtekar KT, Bhalla V, Santos J, Bryce MR, Monkman AP. Triplet harvesting with 100% efficiency by way of thermally activated

- delayed fluorescence in charge transfer OLED emitters. *Advanced Materials*. 2013;
25(27):3707-3714. DOI: 10.1002/adma.201300753
- [46] Chen XK, Zhang SF, Fan JX, Ren AM. Nature of highly efficient thermally activated delayed fluorescence in organic light-emitting diode emitters: Nonadiabatic effect between excited states. *The Journal of Physical Chemistry C*. 2015;**119**(18):9728-9733. DOI: 10.1021/acs.jpcc.5b00276
- [47] Etherington MK, Gibson J, Higginbotham HF, Penfold TJ, Monkman AP. Revealing the spin-vibronic coupling mechanism of thermally activated delayed fluorescence. *Nature Communications*. 2016;**7**. DOI: 10.1038/ncomms13680
- [48] Wu S, Aonuma M, Zhang Q, Huang S, Nakagawa T, Kuwabara K, Adachi C. High-efficiency deep-blue organic light-emitting diodes based on a thermally activated delayed fluorescence emitter. *Journal of Materials Chemistry C*. 2014;**2**(3):421-424. DOI: 10.1039/C3TC31936A
- [49] Rajamalli P, Senthilkumar N, Gandeepan P, Huang PY, Huang MJ, Ren-Wu CZ, Yang CY, Chiu MJ, Chu LK, Lin HW, Cheng CH. A new molecular design based on thermally activated delayed fluorescence for highly efficient organic light emitting diodes. *Journal of the American Chemical Society*. 2016;**138**(2):628-634. DOI: 10.1021/jacs.5b10950
- [50] Kim M, Jeon SK, Hwang SH, Lee JY. Stable blue thermally activated delayed fluorescent organic light-emitting diodes with three times longer lifetime than phosphorescent organic light-emitting diodes. *Advanced Materials*. 2015;**27**(15):2515-2520. DOI: 10.1002/adma.201500267
- [51] Lee DR, Kim M, Jeon SK, Hwang SH, Lee CW, Lee JY. Design strategy for 25% external quantum efficiency in green and blue thermally activated delayed fluorescent devices. *Advanced Materials*. 2015;**27**(39):5861-5867. DOI: 10.1002/adma.201502053
- [52] Lin TA, Chatterjee T, Tsai WL, Lee WK, Wu MJ, Jiao M, Pan KC, Yi CL, Chung CL, Wong KT, Wu CC. Sky-blue organic light emitting diode with 37% external quantum efficiency using thermally activated delayed fluorescence from spiroacridine-triazine hybrid. *Advanced Materials*. 2016;**28**(32):6976-6983. DOI: 10.1002/adma.201601675
- [53] Komatsu R, Sasabe H, Seino Y, Nakao K, Kido J. Light-blue thermally activated delayed fluorescent emitters realizing a high external quantum efficiency of 25% and unprecedented low drive voltages in OLEDs. *Journal of Materials Chemistry C*. 2016;**4**(12):2274-2278. DOI: 10.1039/C5TC04057D
- [54] Sun JW, Kim KH, Moon CK, Lee JH, Kim JJ. Highly efficient sky-blue fluorescent organic light emitting diode based on mixed cohost system for thermally activated delayed fluorescence emitter (2CzPN). *ACS Applied Materials & Interfaces*. 2016;**8**(15):9806-9810. DOI: 10.1021/acsami.6b00286
- [55] Cho YJ, Chin BD, Jeon SK, Lee JY. 20% external quantum efficiency in solution-processed blue thermally activated delayed fluorescent devices. *Advanced Functional Materials*. 2015;**25**(43):6786-6792. DOI: 10.1002/adfm.201502995

- [56] Hatakeyama T, Shiren K, Nakajima K, Nomura S, Nakatsuka S, Kinoshita K, Ni J, Ono Y, Ikuta T. Ultrapure blue thermally activated delayed fluorescence molecules: Efficient HOMO–LUMO separation by the multiple resonance effect. *Advanced Materials*. 2016;**28**(14):2777-2781. DOI: 10.1002/adma.201505491
- [57] Taneda M, Shizu K, Tanaka H, Adachi C. High efficiency thermally activated delayed fluorescence based on 1, 3, 5-tris (4-(diphenylamino) phenyl)-2, 4, 6-tricyanobenzene. *Chemical Communications*. 2015;**51**(24):5028-5031. DOI: 10.1039/C5CC00511F
- [58] Xiang Y, Gong S, Zhao Y, Yin X, Luo J, Wu K, Lu ZH, Yang C. Asymmetric-triazine-cored triads as thermally activated delayed fluorescence emitters for high-efficiency yellow OLEDs with slow efficiency roll-off. *Journal of Materials Chemistry C*. 2016;**4**(42):9998-10004. DOI: 10.1039/C6TC02702D
- [59] Tang C, Yang T, Cao X, Tao Y, Wang F, Zhong C, Qian Y, Zhang X, Huang W. Tuning a weak emissive blue host to highly efficient green dopant by a CN in tetracarbazolepyridines for solution-processed thermally activated delayed fluorescence devices. *Advanced Optical Materials*. 2015;**3**(6):786-790. DOI: 10.1002/adom.201500016
- [60] Tanaka H, Shizu K, Miyazaki H, Adachi C. Efficient green thermally activated delayed fluorescence (TADF) from a phenoxazine–triphenyltriazine (PXZ–TRZ) derivative. *Chemical Communications*. 2012;**48**(93):11392-11394. DOI: 10.1039/C2CC36237F
- [61] Wada Y, Shizu K, Kubo S, Suzuki K, Tanaka H, Adachi C, Kaji H. Highly efficient electroluminescence from a solution-processable thermally activated delayed fluorescence emitter. *Applied Physics Letters*. 2015;**107**(18):105_1. DOI: 10.1063/1.4935237
- [62] Wang H, Xie L, Peng Q, Meng L, Wang Y, Yi Y, Wang P. Novel thermally activated delayed fluorescence materials–thioxanthone derivatives and their applications for highly efficient OLEDs. *Advanced Materials*. 2014;**26**(30):5198-5204. DOI: 10.1002/adma.201401393
- [63] Lee J, Shizu K, Tanaka H, Nomura H, Yasuda T, Adachi C. Oxadiazole-and triazole-based highly-efficient thermally activated delayed fluorescence emitters for organic light-emitting diodes. *Journal of Materials Chemistry C*. 2013;**1**(30):4599-4604. DOI: 10.1039/C3TC30699B